DRAFT VERSION FEBRUARY 3, 2011
Preprint typeset using LaTeX style emulateapj v. 03/07/07

FALL-BACK DISKS IN LONG AND SHORT GRBS

J. K. CANNIZZO[1,2], E. TROJA[3,2], AND N. GEHRELS[2]

Draft version February 3, 2011

ABSTRACT

We present numerical time-dependent calculations for fall-back disks relevant for GRBs in which the disk of material surrounding the black hole (BH) powering the GRB jet modulates the mass flow, and hence the strength of the jet. Given the initial existence of a small mass $\lesssim 10^{-4}M_{\odot}$ near the progenitor with a circularization radius $\sim 10^{10} - 10^{11}$ cm, an unavoidable consequence will be the formation of an "external disk" whose outer edge continually moves to larger radii due to angular momentum transport and lack of a confining torque. For long GRBs, if the mass distribution in the initial fall-back disk traces the progenitor envelope, then a radius $\sim 10^{11}$ cm gives a time scale $\sim 10^4$ s for the X-ray plateau. For late times $t > 10^7$ s a steepening due to a cooling front in the disk may have observational support in GRB 060729. For short GRBs, one expects most of the mass initially to lie at small radii $< 10^8$ cm; however the presence of even a trace amount $\sim 10^{-9}M_{\odot}$ of high angular material can give a brief plateau in the light curve.

Subject headings: gamma rays: bursts

1. INTRODUCTION

The tentative pre-*Swift* hints that breaks occur in the long-term afterglow light curves in different wavebands at $\sim 1-10$ d (Frail et al. 2001) after the GRB have not been borne out by numerous detailed observations of *Swift* GRB afterglows in recent years (Ghisellini et al. 2007, Oates et al. 2007, Racusin et al. 2008, Liang et al. 2008). With *Swift* (Gehrels et al. 2004), the long-term ($t \gtrsim 10^6$ s) X-ray behavior has turned out to be surprisingly complex, exhibiting alternating steep and shallow slopes when plotted as $\log F_x$ versus $\log(t - T0)$ (Zhang et al. 2006; Nousek et al. 2006). Recent workers have begun to explore the possibility that the long-term decay of the X-ray flux is not due to the deceleration of baryonic ejecta, but rather a secular decrease in the rate of accretion powering the central engine, and therefore indirectly the jet (Kumar et al. 2008a, 2008b, Metzger et al. 2008, Cannizzo & Gehrels 2009, hereafter CG09). For long GRBs (lGRBs), the early, steep rate of decay may be giving us information about the radial density distribution within the progenitor core (Kumar et al. 2008b), whereas the later decay may be governed by the outward expansion of the transient disk formed from the remnants of the progenitor CG09).

As regards short GRBs (sGRBs), even if a small amount of material ($\sim 10^{-5} - 10^{-4}M_{\odot}$) is expelled during the NS-NS merger and later accreted in a disk, that would be sufficient to power a bright afterglow, which may also be strongly influenced by the effects of r-process nucleosynthetic heating in the neutron rich material that becomes the disk (Metzger et al. 2010).

Zhang et al. (2006) present a schematic for the decaying GRB light curve as seen by the XRT on *Swift*. The decay is traditionally shown in $\log F - \log t$. There are four basic power-law decay ($F \propto t^{-\alpha}$) regimes: (i) a steep decline following the prompt emission with $\alpha_{\rm I} \simeq 3$ out to $10^2 - 10^3$ s, (ii) a plateau with $\alpha_{\rm II} \simeq 0.5$ out to $10^3 - 10^4$ s, (iii) a steepening with $\alpha_{\rm III} \simeq 1.2$ out to $10^4 - 10^5$ s, and (iv) a further steepening at late times (not always seen) with $\alpha_{\rm IV} \simeq 2$.

CG09 present a general analytical formalism to explain the different power law decays using a fall-back disk, where the variations in α could potentially be accounted for by different physics operating within the disk. The results of CG09 were purely analytical; in this work we present time dependent numerical calculations in order to examine in more detail the potential of the model, and we apply the results to XRT data for one lGRB and one sGRB, taking the best studied of each class. In Section 2 we review the Dainotti relation, an empirical relation involving the duration and luminosity of segment II, in Section 3 we present our detailed numerical model, in Section 4 we compare the model with observations for the lGRB 060729, the GRB with the longest observational time series in X-rays, in Section 5 we compare theory and data for the sGRB 051221A, the sGRB with the longest and most detailed XRT light curve, in Section 6 we revisit the Dainotti relation, in the context of our numerical results, and in Section 7 we discuss and summarize our results.

2. THE DAINOTTI RELATION

Dainotti et al. (2008, 2010) found an empirical relation between the duration of the X-ray plateau in the source frame $t^*_{\rm II} = t_{\rm II}(1+z)^{-1}$, and the X-ray luminosity at the end of the plateau, also corrected into the source frame, $L^*_{\rm II}$. Expressing their relation in the form $\log_{10} L^*_{\rm II}({\rm erg\ s^{-1}}) = a + b \log_{10} t^*_{\rm II}({\rm s})$, Dainotti et al. (2010) find $a = 51.1 \pm 1$ and $b = -1.1 \pm 0.3$. Using the same sample of 62 lGRBs with small errors taken from Dainotti et al. (2010) we find [4] $a = 50.5 \pm 0.4$ and $b = -0.92 \pm 0.1$, close to their results.

If the inverse relation between $L^*_{\rm II}$ and $t^*_{\rm II}$ is physical, and if long-term accretion is the correct explanation for the long-term X-ray light curve of GRBs, that would have implications for the amount of mass in the initial fall-back disk. To first order, the fact that $L^*_{\rm II} t^*_{\rm II}$ is constant would imply the accreted mass reservoir is constant. Willingale et al. (2007) present a

[1] CRESST/Joint Center for Astrophysics, University of Maryland, Baltimore County, Baltimore, MD 21250; John.K.Cannizzo@nasa.gov
[2] Astrophysics Science Division/Code 661/NASA-Goddard Space Flight Center, Greenbelt, MD 20771
[3] NASA Postdoctoral Program

[4] We employ a different method than Dainotti et al. (2010), a Monte Carlo technique in which 10^6 data sets are created with 1σ errors randomly either added or subtracted to each data point in both x and y directions. Thus for N data points one could in principle have N^4 distinct data sets. For each data set, a and b values are calculated, and the final values for a, δa, b, and δb are taken from the averages and standard deviations of the 10^6 values.

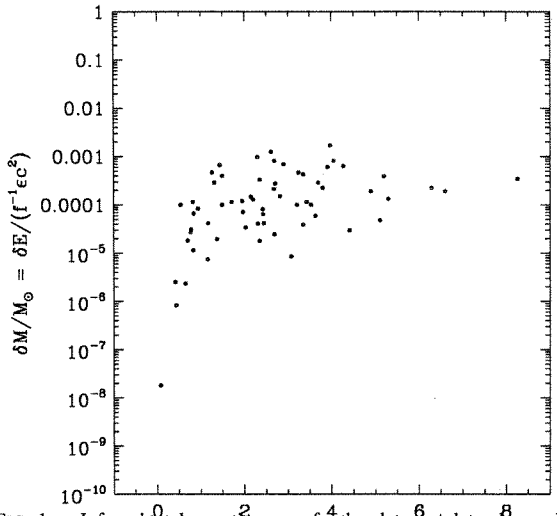

FIG. 1.— Inferred total accretion mass for the plateau + later decay phases of GRBs, using data from Dainotti et al. (2010) for their 62 well-constrained lGRBs. The hatched area (shown in red) indicates a putative limiting XRT detection flux level $f_{\rm II} = 10^{-12}$ erg cm^{-1} s^{-1} (adopting a plateau duration $t_{\rm II} = 10^4$ s) for being able to study a plateau to sufficient accuracy that it would have been included in the Dainotti et al. sample of 62 GRBs with good statistics (i.e., $u \equiv [(\delta \log L^*_{\rm II})^2 + (\delta \log t^*_{\rm II})^2]^{1/2} < 4$) and known redshifts. We adopt a beaming factor $f = 1/300$ and an accretion efficiency for powering the X-ray flux $\epsilon_{\rm acc} = 0.03$ to convert from X-ray fluence (i.e., total X-ray energy, after taking into account $4\pi d_L^2$) to accreted mass.

simple formalism for integrating the X-ray flux on the plateau and subsequent $\alpha_{\rm III} \simeq 1.3$ decay to obtain a total energy. We can convert this into a mass by making a few plausible assumptions about the energetic efficiencies (Krolik, Hawley, & Hirose 2007), e.g., an X-ray afterglow beaming factor $f \simeq 10^{-3} - 10^{-2}$, and an efficiency $\epsilon_{\rm acc} \simeq 0.01 - 0.1$ with which accretion onto the inner engine powers the observed X-rays, presumed to be created within the beamed jet. We use eqns. [3] and [4]) from Willingale et al. (2007) to obtain a total energy δE_X and hence δM derived from the X-ray fluence. The results are shown in Figure 1. The red hatched area indicates The hatched area is bounded from above by an estimate of the effective limiting XRT flux[5] for being able to observe and characterize plateaus sufficiently well that they would satisfy $u < 4$. There appears to be a selection effect giving the Dainotti relation, namely the flux detection limit for XRT prevents one from observing faint plateaus at high z. The Dainotti relation, effectively equivalent to $L^*_{\rm II}t^*_{\rm II} \simeq$ constant, results from the sampling of GRBs primarily beyond $z \simeq 1.5$, for which faint plateaus are observationally biased against. Thus we are seeing basically a narrow strip corresponding to the upper end of a much broader distribution, which makes it appear that $L^*_{\rm II}t^*_{\rm II} \simeq$ constant. For $z \lesssim 1.5$ one sees curvature in the lower envelope of δE_X values due to the strong dependence of the detection limit on z. Nevertheless, the fact that there appears to be a well-defined upper limit $\delta M \approx 10^{-4} - 10^{-3} M_\odot$ is interesting: if one starts with a $\sim 100 M_\odot$ progenitor and if accretion governs the long-term X-ray light curve, this indicates that no more than a fraction $\sim 10^{-6} - 10^{-5}$ of the progenitor mass survives the hypernova to form a fall-back disk.

[5] Our adopted XRT plateau detection level 10^{-12} erg cm^{-1} s^{-1} significantly exceeds the nominal single pointing detection limit $\sim 10^{-14}$ erg cm^{-1} s^{-1} because one must take into account the effect of *Swift* orbital gaps, and also the need to distinguish the different phases of the canonical light curve (i.e., plateau versus steep decay). In addition, the presence of flares may further complicate the picture, but they usually are confined to $t \lesssim 10^3$ s and generally do not represent a major portion of the total energy budget.

3. ACCRETION DISK PHYSICS

By writing the equations for mass continuity and angular momentum transport in cylindrical coordinates, assuming Keplerian rotation $\Omega_K^2 = GM_{\rm BH}r^{-3}$ and integrating over the vertical thickness of the accretion disk, one arrives at an equation for the evolution of the surface density $\Sigma = 2\rho h$, where ρ is the density and h the disk semithickness (actually pressure scale height),

$$\frac{\partial \Sigma}{\partial t} = \frac{3}{r}\frac{\partial}{\partial r}\left[r^{1/2}\frac{\partial}{\partial r}\left(\nu \Sigma r^{1/2}\right)\right]. \quad (1)$$

The kinematic viscosity coefficient

$$\nu = \frac{2\alpha P}{3\Omega_K \rho}, \quad (2)$$

where P is the pressure and α is the Shakura-Sunyaev parametrization of the angular momentum transport and heating (Shakura & Sunyaev 1973). Equation (1) is discretized following the method of Bath & Pringle (1981), in which grid points are distributed as $r^{1/2}$. In addition, one has a thermal energy equation governing the temperature evolution,

$$\frac{\partial T}{\partial t} = \frac{2(A - B + C + D)}{c_p \Sigma} - \frac{\mathcal{R}T}{\mu c_p}\frac{1}{r}\frac{\partial}{\partial r}(r v_r) - v_r \frac{\partial T}{\partial r}, \quad (3)$$

where the viscous heating $A = (9/8)\nu\Omega^2\Sigma$, the radiative cooling $B = \sigma T_e^4$, and C and D represent radial heat fluxes due to turbulent and radiative transport (Cannizzo et al. 2010). For the calculations we present in this work, the thermal equation only becomes of potential importance at very late times > 1 yr.

CG09 present analytical models for the afterglow light curves powered by fall-back disks. The main strength of model is the universal decay law $d\log L_{\rm acc}/d\log t \simeq -1.3$ characterizing fall-back disks without the external, confining tidal torque of a companion star (Cannizzo et al. 1990). This law seems consistent with the late time decay of GRBs seen in X-rays. The early time decay, in particular the steep decay for $t \lesssim 10^3$ s, following the prompt emission, is difficult to explain within the fall-back disk scenario and may be giving us information about the radial density profile within the progenitor (Kumar et al. 2008b). In this work we present results of time dependent numerical calculations using a general accretion disk code (Cannizzo et al. 2010), which uses the input physics detailed in CG09. The boundary conditions are as follows: (i) at the inner disk edge, taken to be 10^7 cm for sGRBs and 10^8 cm for lGRBs, matter is instantly removed as it arrives, while (ii) the outer grid point is placed at such a large radius, typically 10^{13} cm, that during the course of the run the outer edge of the spreading fall-back disk never reaches it. The large dynamic range in disk radii $r_{\rm outer}/r_{\rm inner}$ necessitates $\sim 1500 - 3000$ grid points. In addition, no fresh material is added during a run. Thus the evolution is set entirely by gradients within the disk, unlike the standard Shakura-Sunyaev disk fed at a constant rate in the outer edge which approaches a steady-state $\dot{M}(r) =$ constant with time.

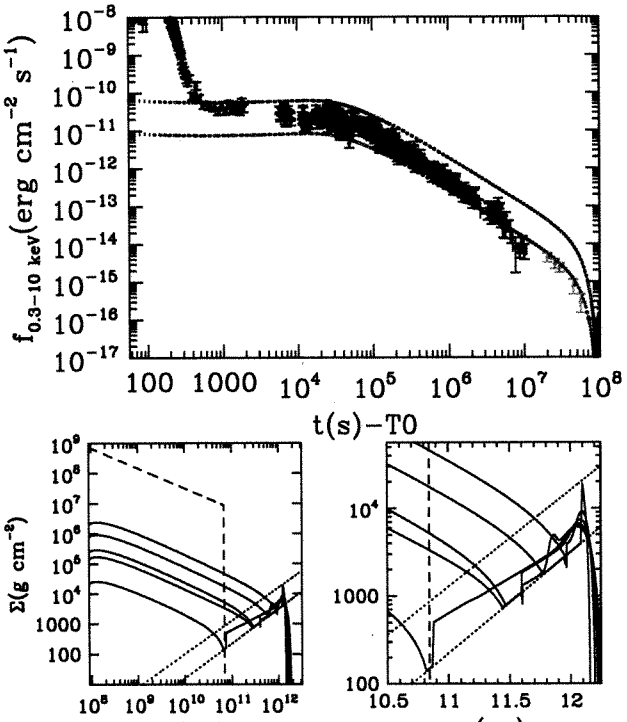

FIG. 2.— Model light curve showing the accretion-derived X-ray flux from the fall-back disk in a lGRB, taking $M_{\rm BH} = 15M_\odot$ and $M_{\rm disk} = 10^{-4}M_\odot$. Also shown is the *Swift* XRT light curve (Evans et al. 2007, 2009) of GRB 060729 (in blue). Given the value $4\pi d_L^2 = 1.15 \times 10^{57}$ cm^2 for GRB 060729 ($z = 0.54$), the efficiencies assumed in the two scaled model light curves (in red) to convert from rate of accretion onto the central engine to XRT fluxes are $f\epsilon_{\rm acc}^{-1} = 8.8 \times 10^{-3}$ (upper) and 1.4×10^{-2} (lower). The five flux values at late times 10^7 s $< t < 10^8$ s (in green) come from *Chandra* observations (Grupe et al. 2010). The last data point lies at $t - T0 = 642$ d. The flat decay portion in the model light curve corresponds to the time during which the initial $\Sigma(r)$ is being redistributed into an accretion disk with a self-consistent radial profile. The bottom panels show $\Sigma(r)$ (solid lines, top to bottom) at $t = 5$, 25, 100, 300, and 600 d. The dashed line indicates the initial $\Sigma(r)$ distribution, and the parallel dotted lines indicate the critical values associated with the dwarf nova limit cycle which occurs at the transition between neutral and ionized gas.

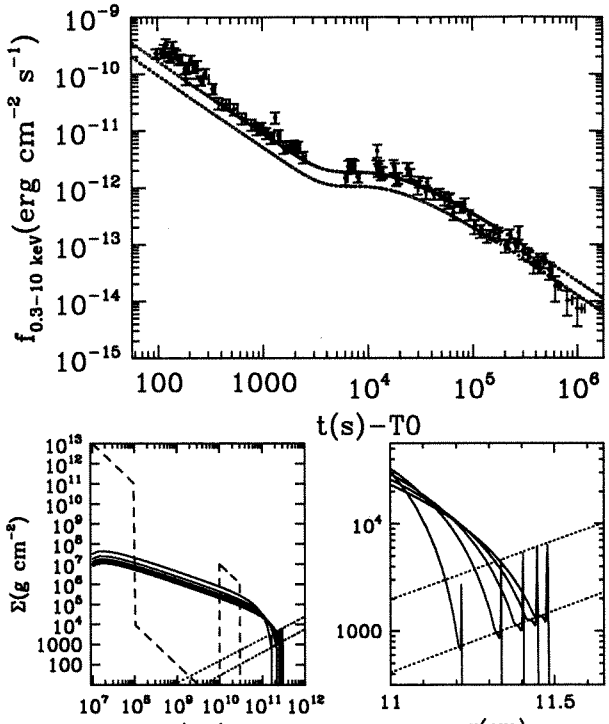

FIG. 3.— Model light curve showing the accretion-derived jet power from the fall-back disk in a sGRB, taking $M_{\rm BH} = 3M_\odot$ and $M_{\rm disk} = 10^{-5}M_\odot$. Also shown is the *Swift* XRT light curve (Evans et al. 2007, 2009) of GRB 051221A (in blue). Given the value $4\pi d_L^2 = 1.18 \times 10^{57}$ cm^2 for GRB 051221A ($z = 0.5465$), the efficiencies assumed in the two scaled model light curves (in red) to convert from rate of accretion onto the central engine to XRT fluxes are $f\epsilon_{\rm acc}^{-1} = 2.4 \times 10^{-2}$ (upper) and 4.3×10^{-2} (lower). One sees fairly rapid decay initially due to the presence of a significant amount of accreting material at small radii. The brief shoulder in the light curve is due to the delayed accretion of the spiral arm of ejected NS matter at large radii, motivated by detailed SPH calculations (Rosswog 2007). The bottom panels show the surface density evolution, at equally spaced intervals $\delta t = 2$ d. The dashed line indicates the initial $\Sigma(r)$ distribution, and the parallel dotted lines indicate the critical values associated with the dwarf nova limit cycle.

4. LGRBS

LGRBs are thought to be due to the explosion of a short-lived $\gtrsim 30M_\odot$ progenitor (MacFadyen & Woosley 1999). The hosts for lGRBs tend to be subluminous, irregular galaxies rich in star formation (Fruchter, et al. 2006). If the long-term X-ray light curves of GRBs are indicative of feeding from a fall-back accretion disk, then from Figure 1 we see that no more than $\sim 10^{-4} - 10^{-3}M_\odot$ of material in the fall-back disk is needed, for nominal assumptions about the efficiencies. In other words, for a $\sim 100M_\odot$ progenitor, a mass fraction only $\sim 10^{-6} - 10^{-5}$ (excluding the $\sim 10M_\odot$ which ends up within $t \lesssim 10 - 10^2$ s in the BH) is required to survive and persist in the vicinity of the progenitor to power the long-term light curve.

Figure 2 shows a light curve for $M_{\rm BH} = 15M_\odot$ and $M_{\rm disk} = 10^{-4}M_\odot$. The initial $\Sigma(r)$ profile is taken to be $\propto r^{-2/3}$ out to 7×10^{10} cm, and zero for larger radii. The lower panels reveal the $\Sigma(r,t)$ evolution. The steep decay associated with segment I is not accounted for in our model, and may well be due to a separate physical process, such as the accretion of the progenitor core (Kumar et al. 2008b; Lindner et al. 2010, see their Fig. 2). The time scale $t_{\rm II}$ for the plateau associated with segment II comes out naturally in the models, given the $\sim 10^{11}$ cm radius for the progenitor – assuming that the initial fall-back mass distribution roughly traces the envelope of the progenitor. The observed X-ray decay for GRB 060729, the GRB which has the been observed for the longest time in X-rays (Grupe et al, 2007, 2010), does not match precisely that of the fall-back disk. There may be various systematic effects that could account for the difference. The most obvious effect, a variable cosmological K-correction concomitant with the fading in X-ray flux over a dynamic range of ~ 6 decades, cannot play a strong role, as the spectral index does not vary significantly over the long term from its mean value $\beta \simeq 2$. There may be some time-variable physics associated with the X-ray emission from within the jet that could affect either $\epsilon_{\rm acc}$ or f versus time. Our calculations only represent the accretion disk which powers the jet and we take

$\dot{\epsilon}_{\rm acc} = \dot{f} = 0$ for simplicity. Modeling the jet emission is beyond the scope of this work.

At late times 10^7 s $< t < 10^8$ s there is a deviation from the canonical power law decay because $\Sigma(r_{\rm outer})$ drops to the point at which the dwarf nova limit cycle becomes active (indicated by the parallel dashed lines), and a cooling front is launched from the outer edge that instigates a transition from ionized to neutral gas. This quenches the source of accretion onto the central engine. The very late time *Chandra* observations of GRB 060729 (Grupe et al. 2010) appear to coincide with the timing of this drop-off, which may therefore represent a cooling transition front in the outer disk which diminishes the rate of accretion onto the central engine, rather than a jet break.

5. SGRBS

SGRBs are thought to be caused by the merger of two neutron stars (Eichler et al. 1989; Paczyński 1991; Narayan, Piran, & Kumar 2001; Rosswog & Ramirez-Ruiz 2002). The hosts for sGRBs tend to be ~ 5 times more spatially extended than those for lGRBs (matching the ~ 5 times wider projected spatial distribution of sGRBs vs. lGRBs within their hosts), are also more indicative of an older population with less active star formation (Fong, Berger, & Fox 2010). Due to their faintness relative to lGRBs, sGRBs are much less well-studied in X-rays. Indeed, there is only one certifiable example of a sGRB which has a long and well-sampled X-ray light curve, to the extent that a statement can be made as to the presence of a plateau - GRB 051221A.

The importance of the outward spreading of the disk formed from the NS-NS merger was clearly demonstrated by Metzger et al. (2008, see their Fig. 1). The initial radial density profile, and hence $\Sigma(r)$ profile after after angular momentum conservation has vertically compacted the merger remnants into their accretion plane, is of course much more compact radially than that expected for lGRBs. Theoretical guidance on a potential $\Sigma(r)$ profile to begin the calculations, particularly at large radii, is scarce, yet there are indications of small amounts of matter $\sim 10^{-6} - 10^{-4} M_\odot$ ejected at early times that may have high angular momentum, and therefore circularize at large radii (Rosswog 2007).

Figure 3 shows the evolution of a fall-back disk of potential relevance for the aftermath of a NS-NS merger. We take $M_{\rm BH} = 3M_\odot$ and $M_{\rm disk} = 10^{-5} M_\odot$. Unlike the much longer evolution shown in Figure 2 for lGRBs, in this case the outer edge of the disk is still freely expanding to larger radii by the end of the run (indicated by the narrow spike in $\Sigma(r)$ between 10^{11} cm and 3×10^{11} cm shown in the second lower panel). The brief plateau at $\sim 10^4$ s results from the ad hoc introduction of the small amount $\sim 10^{-9} M_\odot$ of high angular momentum material at the large circularization radius 10^{10} cm. The high efficiencies associated with BH accretion show the potential for a small amount of material $\ll 1 M_\odot$ to have a dramatic effect on the long-term light curves as regards brief plateaus or inflection points.

6. POTENTIAL APPLICATION TO A DAINOTTI-LIKE RELATION

In Section 2 we show that the Dainotti relation $L^*_{\rm II} \tilde{\propto} {t^*}^{-1}_{\rm II}$ as originally envisioned may be due to the observational bias against detecting and characterizing faint plateaus. Nevertheless, the accreted mass estimates δM inferred using the $L^*_{\rm II}$ and $t^*_{\rm II}$ values from Dainotti et al. (2010) are interesting in the context of this work, and one might legitimately ask what

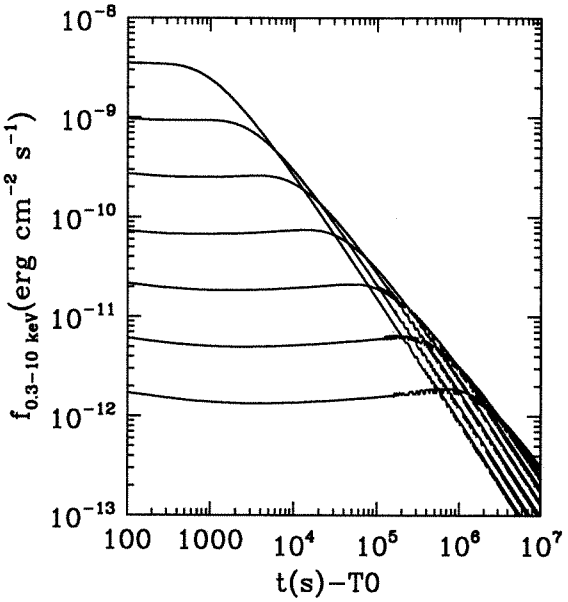

FIG. 4.— Model light curves for lGRB parameters, keeping the initial fall-back disk mass constant at $10^{-4} M_\odot$ but varying the initial radius and overall normalization. For the central light curve $r_0 = 7 \times 10^{10}$ cm, as in Figure 1. For each successive light curve r_0 is increased a factor of two going to the right, and decreased a factor of two going to the left. To keep δM constant, the overall normalization on $\Sigma(0)$ is varied by an additional factor of 2.5 for each successive run.

theoretical prediction for the $L^*_{\rm II}(t^*_{\rm II})$ relation the fall-back accretion hypothesis would make, given a hypothetical physical constraint in which δM were held constant and the initial radius of the fall-back disk were allowed to vary. Figure 4 shows the results of seven runs in which we fix $\delta M = 10^{-4} M_\odot$ and vary the initial outer radius of the fall back disk. One can see a clear inverse relation between the duration of the plateau $t^*_{\rm II}$ and the luminosity at the end of the plateau $L^*_{\rm II}$. The low$-z$ behavior of δM seen in Figure 1, however, indicates that a spread in δM may be more realistic, in which case one would not expect to be able to use the theoretical prediction of the $L^*_{\rm II}(t^*_{\rm II})$ relation as a useful discriminant for the theory.

7. DISCUSSION AND CONCLUSION

We have presented time dependent calculations of the fall-back disk scenario to account for the long-term X-ray light curves for GRBs. For lGRBs, an initial radial scale of a stellar radius $\sim 10^{11}$ gives a natural viscous evolution time of $\sim 10^4$ s to redistribute the matter into a quasi-steady disk, roughly consistent with the observed plateau duration. The rate of decay for GRB 060729 is close but does not match the models precisely, which may hint at time-variable emission processes that would affect our adopted efficiencies $\epsilon_{\rm acc}$ and f. It is interesting to note that our effective values of the efficiencies, accretion plus beaming, required to match the observed X-ray flux levels are comparable between lGRBs and sGRBs: $f\epsilon^{-1}_{\rm acc} \simeq 10^{-2}$ for GRB 060729 and $f\epsilon^{-1}_{\rm acc} \simeq 3 \times 10^{-2}$ for GRB 051221A. If the accretion efficiency $\epsilon_{\rm acc}$ is about the same for lGRBs and sGRBs, this may indicate that sGRBs are less beamed by a factor of ~ 3 compared to lGRBs, roughly in line with previous results (Watson et al. 2006, Grupe et al. 2006). This similarity between lGRBs and sGRBs afterglows

is not entirely unexpected, given the general similarities in their afterglow properties (Gehrels et al. 2008; Nysewander, Fruchter, & Pe'er 2009).

At very late times *Chandra* observations indicate a steepening in the rate of decay (Grupe et al. 2010), which appears to be consistent with the onset of a cooling front in the disk. This would be an alternative to the standard jet-break interpretation discussed by Grupe et al. (2010). For sGRBs, the picture is less clear, given that we only have a single well-studied example. We have shown that the presence of even a very small amount of high angular momentum gas $\sim 10^{-9}M_{\odot}$ can give a slight inflection to the X-ray decay, as was observed in GRB 051221A. If only $\sim 10^{-4}M_{\odot}$ of gas survives either the hypernova (lGRBs) or NS-NS merger (sGRBs), then the accretion resulting from the ensuing fall-back disk should power a long-term jet.

Lastly, we have shown that the Dainotti relation $L^{*}_{\rm II} \widetilde{\propto} t^{*-1}_{\rm II}$ may be due to an observational bias against detecting and characterizing faint plateaus: the relation is governed by GRBs at $z \gtrsim 1.5$ for which we only detect the upper envelope of a broad distribution. Nevertheless, the existence of an apparent upper limit to the total X-ray energies inferred from the X-ray fluences, and therefore the accreted masses if one assumes accretion onto the central engine as the long term powerhouse for the X-ray flux, is extremely interesting. For nominal values of the accretion efficiency $\epsilon_{\rm acc}$ and the beaming factor f, we find an upper limit $\simeq 10^{-4} - 10^{-3}M_{\odot}$ for the accreted masses. (The lower end of the distribution of accreted masses, which is partially revealed for GRBs at $z \lesssim 1.5$, may extend down to $\simeq 10^{-8} - 10^{-7}M_{\odot}$.) This means that for a progenitor mass $\sim 100M_{\odot}$, only a maximum mass fraction $\sim 10^{-6} - 10^{-5}$ of the progenitor survives in the vicinity of the progenitor to be accreted as a fall-back disk (excluding the $\sim 10M_{\odot}$ that ends up in the BH during the prompt emission and subsequent segment I consisting of the steep-decay). This has important ramifications for the energetics associated with the hypernova explosion and subsequent removal of most of the progenitor envelope.

We acknowledge useful conversations with Maria Dainotti, Stephan Rosswog, and Brad Schaefer. This work made use of data supplied by the UK *Swift* Science Data Centre at the University of Leicester.

REFERENCES

Bath, G. T., & Pringle, J. E. 1981, MNRAS, 194, 967
Cannizzo, J. K., & Gehrels, N. 2009, ApJ, 700, 1047 (CG09)
Cannizzo, J. K., Lee, H.-M., & Goodman, J. 1990, ApJ, 351, 38
Cannizzo, J. K., Still, M. D., Howell, S. B., Wood, M. A., & Smale, A. P. 2010, ApJ, 725, 1393
Dainotti, M. G., Cardone, V. F., Capozziello, S. 2008, MNRAS, 391, L79
Dainotti, M. G., Willingale, R., Capozziello, S., Cardone, V. F., & Ostrowski, M. 2010, ApJ, 722, L215
Eichler, D., Livio, M., Piran, T., & Schramm, D. N. 1989, Nature, 340, 126
Evans, P. A., et al. 2007, A&A, 469, 379
Evans, P. A., et al. 2009, MNRAS, 397, 1177
Fong, W., Berger, E., & Fox, D. B. 2010, ApJ, 708, 9
Frail, D. A., et al. 2001, ApJ, 562, L55
Fruchter, A. S., et al. 2006, Nature, 441, 463
Gehrels, N., et al. 2004, ApJ, 611, 1005
Gehrels, N., et al. 2008, ApJ, 689, 1161
Ghisellini, G., Ghirlanda, G., Nava, L., & Firmani, C. 2007, ApJ, 658, L75
Grupe, D., Burrows, D. N., Patel, S. K., Kouveliotou, C., Zhang, B., Mészáros, P., Wijers, R. A. M., & Gehrels, N. 2006, ApJ, 653, 462
Grupe, D., et al. 2007, ApJ, 662, 443
Grupe, D., et al. 2010, ApJ, 711, 1008
Krolik, J. H., Hawley, J. F., & Hirose, S. 2007, RevMexAA, 27, 1
Kumar, P., Narayan, R., & Johnson, J. L. 2008a, MNRAS, 388, 1729
Kumar, P., Narayan, R., & Johnson, J. L. 2008b, Science, 321, 376
Liang, E.-W., Racusin, J. L., Zhang, B., Zhang, B.-B., & Burrows, D. N. 2008, ApJ, 675, 528
Lindner, C. C., Milosavljević, M., Couch, S. M., & Kumar, K. 2010, ApJ, 713, 800
MacFadyen, A. I., & Woosley, S. E. 1999, ApJ, 524, 262
Metzger, B. D., Arcones, A., Quataert, E., & Martínez-Pinedo, G. 2010, MNRAS, 402, 2771
Metzger, B. D., Piro, A. L., & Quataert, E. 2008, MNRAS, 390, 781
Narayan, R., Piran, T., & Kumar, P. 2001, ApJ, 557, 949
Nousek, J. A., et al. 2006, ApJ, 642, 389
Nysewander, M., Fruchter, A. S., & Pe'er, A. 2009, ApJ, 701, 824
Oates, S. R., et al. 2007, MNRAS, 380, 270
Paczyński, B. 1991, Acta Astr., 41, 257
Racusin, J. L., et al. 2008, Nature, 455, 183
Rosswog, S. 2007, MNRAS, 376, L48
Rosswog, S., & Ramirez-Ruiz, E. 2002, MNRAS, 336, 7
Shakura, N. I., & Sunyaev, R. A. 1973, A&A, 24, 337
Watson, D., Hjorth, J., Jakobsson, P., Xu, D., Fynbo, J. P. U., Sollerman, J., Thöne, C. C., & Pedersen, K. 2006, A&A, 454, L123
Willingale, R., et al. 2007, ApJ, 662, 1093
Zhang, B., et al. 2006, ApJ, 642, 354